JOURNAL OF SOLID STATE CHEMISTRY 73, 252–258 (1988).

Structural Study of $NaNdGa_4S_8$, a Luminescent Material with Low-Concentration Quenching

R. IBANEZ*

Colegio Universitario de Castellón, Universidad de Valencia, Apdo de Correos 224, Castellón, Spain

AND P. GRAVEREAU, A. GARCIA, AND C. FOUASSIER

Laboratoire de Chimie du Solide du CNRS, Université de Bordeaux I, 351, cours de la Libération, 33405 Talence Cedex, France

Received July 8, 1987

Single-crystal X-ray diffraction analysis and optical investigations of $NaNdGa_4S_8$ show that Nd^{3+} ions are essentially distributed in two of the three square antiprismatic sites of a $CaGa_2S_4$-type lattice. The NdS_8 polyhedra are isolated (minimum Nd–Nd distance: 6.07 Å) so the interactions responsible for concentration quenching of the luminescence are considerably reduced.

Introduction

Recently we have reported the luminescence properties of Nd^{3+} in the solid solutions $Na_xNd_xM_{1-2x}Ga_2S_4$ ($x \leq 0.5$; M = Ca,Sr) (*1*). Two remarkable features are a very weak self-quenching of the IR emission and an efficient UV charge transfer band excitation. The limit composition for $x = 0.5$, $NaNdGa_4S_8$, is the first stoichiometric sulfide showing high luminescence efficiency. The quantum yield of the $^4F_{3/2}$ emission is only reduced by 1.3 by intercationic interactions compared to a factor of nearly 3 for the well-known low-concentration quenching phosphate, NdP_5O_{14} (*2*).

One of the main mechanisms responsible for concentration quenching is the cross-relaxation process $^4F_{3/2} \rightarrow {}^4I_{15/2}$, $^4I_{9/2} \rightarrow {}^4I_{15/2}$. The probability of energy transfer is reduced when the splitting of the lowest energy level ($^4I_{9/2}$) is less than 470 cm^{-1} (*3*). The values observed in thiogallates lie well below this limit.

A second condition for low-concentration quenching is a large intercationic distance. The structure of $CaGa_2S_4$ has been recently determined (*4*). The divalent cations occupy three slightly distorted square antiprismatic sites sharing apices and edges. In this paper we present the results of optical and X-ray diffraction investigations which have allowed the determination of the positions of the neodymium ions in the lattice of $NaNdGa_4S_8$.

X-Ray Diffraction Analysis

X-ray Powder Diffraction Pattern

The X-ray diffraction spectrum was obtained with the automated powder diffrac-

* To whom correspondence should be addressed.

0022-4596/88 $3.00

tometer PW 1710 Philips, Cu$K\alpha$ radiation, and silicon standard. As $a \simeq b$, (hkl) and (khl) peaks are not resolved and in a previous attempt lattice parameters were refined in the tetragonal system to the values $a = 20.129(2)$ and $c = 12.141(1)$ Å. Using observed structure factors deduced from the single-crystal diffractometer data collection, 20 reflections with $h \neq k$ could be indexed without ambiguity. Adding 10 indexed (hhl) reflections we have done a least-squares refinement in the orthorhombic system which led to the values $a = 20.122(2)$, $b = 20.143(2)$, $c = 12.142(1)$ Å; $V = 4923.1(8)$ Å^3; $Z = 16$; $d_{calc.} = 3.79$ g · cm^{-3}.

X-ray powder diffraction data are summarized in Table I. The relative intensities were estimated by the peak-to-background height. Value of the quantitative figure of merit defined by Smith and Snyder (*5*), $F_N = (1/|\overline{\Delta 2\theta}|).(N/N_{poss.})$, has been calculated for the 30th observed line ($N = 30$): $F_{30} = 16.5$ ($|\overline{\Delta 2\theta}| = 0.016$, $N_{poss.} = 114$). $|\overline{\Delta 2\theta}|$ is the average of the absolute discrepancy between the observed and calculated 2θ values. $N_{poss.}$ is the number of possible diffraction lines up to the 30th observed. The low value of F_{30} is essentially due to (hkl) and (khl) peaks superposition ($N_{poss.} \gg N$).

Single-Crystal X-ray Study

Single crystals were obtained by fusion and subsequent slow cooling of a powder sample placed in a carbon crucible inside a

TABLE I

$NaNdGa_4S_8$ POWDER DIFFRACTION DATA (Cu$K\alpha$ RADIATION)

$2\theta_{exp}$ (°)	100 I/I_0	d_{exp} (Å)	$h\ k\ l$	$2\theta_{exp}$ (°)	100 I/I_0	d_{exp} (Å)	$h\ k\ l$
12.43	43	7.12	220	46.92	10	1.937	804
17.07	31	5.19	202, 022	47.61	28	1.908	862
17.62	35	5.03	400	48.62	5	1.873	664
19.22	9	4.62	222	49.34	14	1.847	175, 246, 426
22.84	9	3.98	113	50.53	6	1.806	1(11)1
23.68	10	3.76	151	51.10	12	1.788	4(10)2, (10)42, 375
24.61	100	3.62	422	52.32	4	1.747	3(11)1
25.03	21	3.56	440	52.80	6	1.732	066, 606
26.10	6	3.41	313				6(10)0, (10)60
26.83	6	3.22	351	53.64	17	1.707	266, 626
28.04	12	3.18	260, 620	54.74	6	1.676	(12)00
29.42	3	3.04	004	55.30	13	1.660	6(10)2, (10)62
30.42	47	2.938	062	57.93	12	1.591	12(40), 4(12)0+
31.73	43	2.820	262, 622, 153,	59.31	3	1.5569	286, 826, 775
			513	60.24	8	1.5369	884,7(11)1, (11)71
32.08	12	2.790	224	61.02	7	1.5171	008
34.13	4	2.627	353	63.25	5	1.4690	0(12)4
34.66	5	2.588	371	65.33	7	1.4272	866, 686, 975+
35.69	51	2.516	800	66.28	5	1.4089	(12)44,4(12)4
37.95	3	2.371	660	71.82	4	1.3132	(10)66
39.02	71	2.308	444	72.70	5	1.2996	088, 808
39.77	8	2.266	282, 822, 135	73.39	4	1.2890	(10)(12)0, (10)(10)4
40.05	15	2.252	480				288+
41.11	9	2.196	264, 624	74.82	3	1.2690	(12)84, 8(12)4
44.08	6	2.055	644	75.53	5	1.2577	(16)00
46.00	5	1.973	2(10)0, (10)20	87.53	2	1.1136	46(10), 64(10)

sealed quartz tube. The quality of single crystals was tested with X-ray photographs (Weissenberg, precession, . . .) which indicated orthorhombic symmetry with an *F*-centered lattice.

A prismatic single crystal (edge sizes ranging from 40 to 160 μm) was mounted on an automatic three-circle diffractometer (CAD3 Enraf–Nonius). Reflections with *F*-centered conditions (3517) have been collected by the θ–2θ scan technique (sin $\theta/\lambda \leq 0.704$ Å^{-1}, $-28 \leq h \leq 26$, $-8 \leq k \leq 28$, $-16 \leq l \leq 3$), with graphite monochromatized Mo$K\alpha$ radiation ($\lambda = 0.71069$ Å) and with an angular width of $0.70° + 0.60°$ tan θ. After correction by the Lorentz-polarization factor, the reflections were averaged and reduced to 1182 unique reflections with

$$I/\sigma(I) > 2(R_{INT}[\Sigma(\Sigma|F_o - \langle F_o\rangle|)/\Sigma F_o] = 0.033).$$

No absorption corrections were made ($\mu = 14.01$ mm^{-1}). Additional conditions for reflections $k + 1 = 4n$ for $(0kl)$, $h + l = 4n$ for $(h0l)$, and $h + k = 4n$ for $(hk0)$, led to the space group *Fddd* (only five inconsistencies with $2 < I/\sigma(I) < 4$).

All calculations for structure determination were performed with SHELX 76 (*6*). Scattering factors for Na^+, Nd^{3+}, Ga^{3+}, S, and anomalous dispersion corrections were taken from "International Tables for X-Ray Crystallography" (*7*). The above X-ray results confirmed that the crystal structure derived from the structural type of $EuGa_2S_4$ (*8*), $BaIn_2Se_4$ (*9*), $CaGa_2S_4$, and $SrGa_2S_4$ (*4*). In this structure the divalent cations are located on the 8a, 8b, and 16e sites of the *Fddd* group. In the case of $NaNdGa_4S_8$, Na and Nd atoms had to be distributed over these sites. Due to low concentration quenching of the emission it could be assumed that Nd^{3+} ions were lying in sulfur coordination polyhedra devoid of common apices. Two ordered distributions were in agreement with this hypothesis:

I. Nd on 8a and 8b–Na on 16e
II. Nd on 16e–Na on 8a and 8b

Calculations with the 1177 unique reflections and individual isotropic thermal parameters (29 variables) yielded $R[\Sigma|F_o - |F_c||/\Sigma F_o] = 0.08$ and 0.10, respectively, for distributions I and II. Some reflections are insensitive (187 reflections with $h = 2n$ and $h + k + l \neq 4n$) or not very sensitive to the sites permutation I $\rightleftarrows$ II. To enhance the variation, we have calculated *R* for intermediate atomic distributions between I and II, using the 402 reflections for which $|F_{c_I} - F_{c_{II}}|/F_o > 0.30$.

Figure 1 shows the variation of *R* as a function of the fraction (X_{Nd}) of the 16e site occupied by Nd atoms (the distribution of neodymium and sodium atoms on the 8a and 8b sites is assumed to be disordered). From these results,

—the statistical case ($x_{Nd} = 0.50$) can be clearly rejected;
—distribution I is the most likely one;

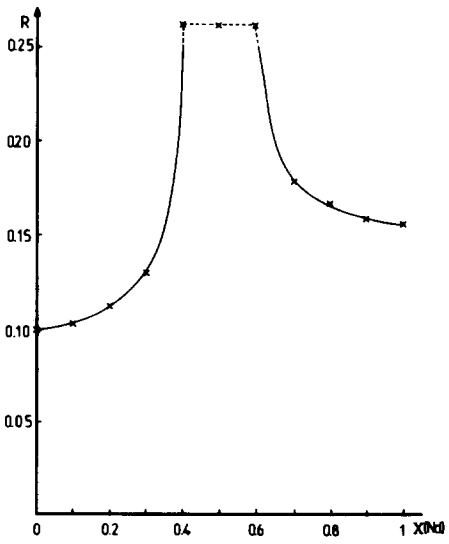

FIG. 1. Variation of the *R* factor as a function of the fraction (x_{Nd}) of the Nd atoms in the 16e site (calculations with a reduced file of selected structure factors).

likewise the obtained isotropic thermal parameters of Na and Nd atoms which have more significant relative values in this case support this conclusion.

Consequently the structural model has been optimized with the distribution I in the following way: 1177 unique reflections, a weighting scheme $\omega = 1/\sigma^2(F_o)$, an empirical isotropic extinction parameter $x(Fc = F(1-10^{-4} \times F^2/\sin\theta))$ and individual anisotropic thermal parameters. The structure was refined to $R = 0.064$ and $\omega R = [\Sigma\omega(F_o - |F_c|)^2/\Sigma\omega F_o^2]^{1/2} = 0.059$, extinction parameter $x = 2 \times 10^{-5}$, shift/e.s.d. in last cycle ≤ 0.001, and residual electron density ranging from -2.5 to $3.8e\ Å^{-3}$ with maxima near Nd and Ga atoms. The atomic parameters are given in Table II and selected bond lengths and angles in Table III (structure factors table will be sent upon request).

Description and Discussion

The two independent neodymium atoms occupy centers of slightly distorted square antiprismatic sulfur polyhedra (222 symmetry) with: $\overline{Nd(1)\text{-}S} = 2.970$ and $\overline{Nd(2)\text{-}S} =$

TABLE II

ATOMIC PARAMETERS[a,b]

A	Atoms	Position	Site symmetry	x	y	z	$B_{eq.}$ (Å²)
	Nd(1)	8a	222	1/8	1/8	1/8	0.68(3)
	Nd(2)	8b	222	1/8	1/8	5/8	0.78(3)
	Na	16e	2..	0.3785(5)	1/8	1/8	2.3 (2)
	Ga(1)	32h	1	0.7527(1)	0.4892(1)	0.1254(1)	0.82(3)
	Ga(2)	32h	1	0.7496(1)	0.6952(1)	0.4140(1)	0.78(3)
	S(1)	32h	1	0.0041(2)	0.5933(2)	0.2514(3)	0.93(7)
	S(2)	32h	1	0.7500(2)	0.5821(2)	0.0156(2)	0.74(7)
	S(3)	32h	1	0.5850(2)	0.7470(2)	0.2446(3)	0.84(7)
	S94)	32h	1	0.9143(2)	0.4977(2)	0.9963(3)	0.89(7)

		$\times 10^4$ (Å²)					
B	Atoms	U_{11}	U_{22}	U_{33}	U_{23}	U_{13}	U_{12}
	Nd(1)	107(7)	48(6)	102(7)	0	0	0
	Nd(2)	131(7)	63(7)	102(7)	0	0	0
	Na	193(38)	318(46)	351(45)	−32(46)	0	0
	Ga(1)	152(7)	67(7)	91(6)	−7(6)	3(9)	12(5)
	Ga(2)	153(7)	65(7)	79(6)	−5(6)	8(6)	−5(5)
	S(1)	179(18)	55(16)	120(15)	22(12)	36(14)	−15(13)
	S(2)	176(18)	47(14)	58(15)	1(11)	1(13)	6(12)
	S(3)	123(17)	93(15)	103(16)	−17(12)	17(13)	34(13)
	S(4)	130(17)	90(16)	119(16)	3(13)	20(14)	−5(13)

[a] Position, site symmetry, fractional coordinates, and equivalent values of isotropic temperature factors (calculated as $B_{eq.} = \frac{8\pi^2}{3}\sum_{i=1}^{3}\sum_{j=1}^{3} a_i^* a_j^* U_{ij}(\mathbf{a}_i \cdot \mathbf{a}_j)$.

[b] Anisotropic thermal parameters of temperature factors; $T = \exp[-2\pi^2(h^2a^{*2}U_{11} + k^2b^{*2}U_{22} + l^2c^{*2}U_{33} + 2klb^*c^*U_{23} + 2lhc^*a^*U_{13} + 2hka^*b^*U_{12})]$.

TABLE III

SELECTED INTERATOMIC DISTANCES (Å) AND ANGLES (°) FOR THE COORDINATION POLYHEDRA (e.s.d. IN PARENTHESES)

Nd(1)–S(2)(×4) 2.973(3)	Na–S(1)(×2) 3.025(9)
Nd(1)–S(3)(×4) 2.966(3)	Na–S(2)(×2) 3.033(9)
	Na–S(3)(×2) 3.150(5)
Nd(2)–S(1)(×4) 2.947(3)	Na–S(4)(×2) 3.088(4)
Nd(2)–S(4)(×4) 2.983(3)	
Ga(1)–S(1) 2.241(3)	S(1)–Ga(1)–S(2) 102.3(2)
Ga(1)–S(2) 2.298(3)	S(1)–Ga(1)–S(3) 120.3(2)
Ga(1)–S(3) 2.293(3)	S(1)–Ga(1)–S(3')121.5(2)
Ga(1)–S(3')2.299(3)	S(2)–Ga(1)–S(3) 111.1(2)
	S(2)–Ga(1)–S(3')104.4(2)
	S(3)–Ga(1)–S(3') 96.5(2)
Ga(2)–S(1) 2.298(3)	S(1)–Ga(2)–S(2) 102.4(2)
Ga(2)–S(2) 2.249(3)	S(1)–Ga(2)–S(4) 106.0(2)
Ga(2)–S(4) 2.307(3)	S(1)–Ga(2)–S(4')100.1(2)
Ga(2)–S(4')2.291(3)	S(2)–Ga(2)–S(4) 122.6(2)
	S(2)–Ga(2)–S(4')125.2(2)
	S(4)–Ga(2)–S(4') 97.3(2)

2.965 Å. These polyhedra are isolated from one another so the repulsion between Nd^{3+} ions, as well as the probability of the various mechanisms responsible for nonradiative losses (*10, 11*) are minimized.

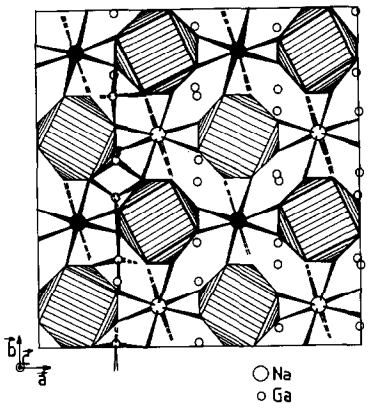

FIG. 2. Projection of the lower half of the unit cell along [001]. The hatched polyhedra correspond to Nd antiprisms centered at z = 1/8 (*light marking*) *or* z = 3/8 (heavy marking). The large circles represent the sodium sites at z = 1/8 (open circles) and 3/8 (shaded circles). The small circles correspond to gallium atoms.

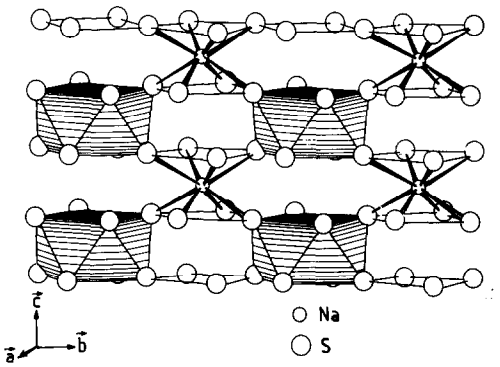

FIG. 3. Assembly of the Nd and Na antiprisms in plane parallel to (100).

Sodium ions have quite similar square antiprismatic sulfur environment (2.. symmetry) with Na-S = 3.074 Å. Figures 2 and 3 show the assembly of (NdS_8) and (NaS_8) polyhedra in planes parallel to (001) and (100), respectively. In the [100] direction each Nd antiprism shares two edges with two Na antiprisms, along the twofold axes. Other corners are shared with four other Na antiprisms.

Gallium ions are nearly disposed in planes parallel to (100). They have tetrahedral sulfur environment with important angular distortions around the ideal value (109.47°): 96.5–121.5° and 97.3–125.2° for Ga(1) and Ga(2), respectively. Figure 4

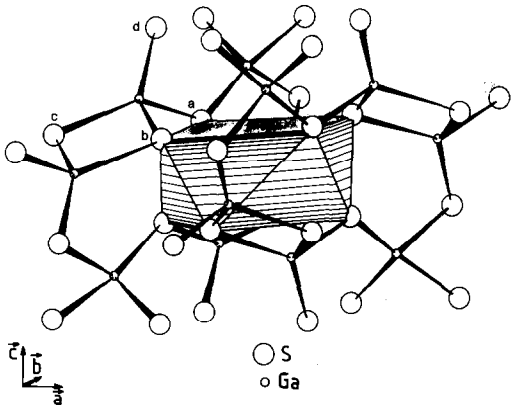

FIG. 4. Arrangement of the (GaS_4) tetrahedra around a (NdS_8) antiprism.

shows the arrangement of Ga tetrahedra around a Nd antiprism. If we call "*a*," "*b*," "*c*," and "*d*" the vertices of a (GaS_4) tetrahedron a qualitative explanation for the observed distortions can be given. An edge (*a*–*b*) is shared with a Nd antiprism, a second edge (*b*–*c*) is shared with another Ga tetrahedron, and the fourth vertex (*d*) is shared with a third Ga tetrahedron. As cation–cation repulsion is stronger for polyhedra connected by edges than for polyhedra joined by a corner, Ga-*a*, Ga-*b*, Ga-*c* lengths (mean values 2.297 and 2.299 Å for Ga(1) and Ga(2) are greater than Ga-*d* lengths (2.241 and 2.249 Å for Ga(1) and Ga(2)). Low values of *b*-Ga-*c* angles (96.5° and 97.3° for Ga(1) and Ga(2) and to a lesser extent of *a*-Ga-*b* angles (104.4° and 100.1° for Ga(1) and Ga(2)) also contribute to reduce the gallium–gallium and gallium–neodymium repulsions, respectively.

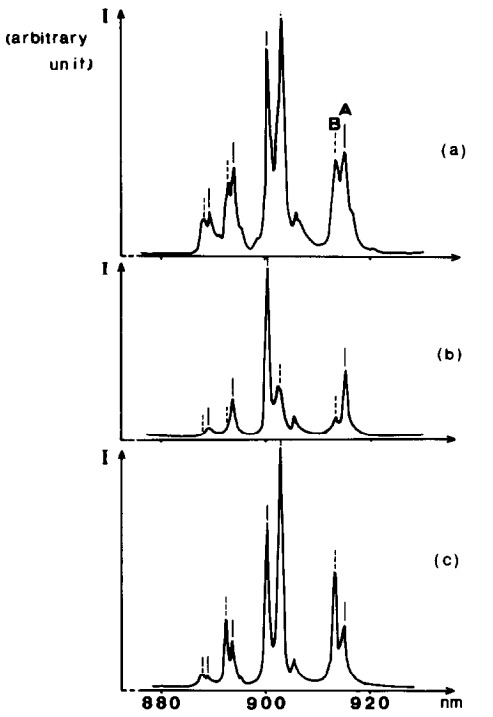

FIG. 5. $^4F_{3/2} \rightarrow {}^4I_{9/2}$ emission of Nd^{3+} in $NaNdGa_4S_8$ for excitation into the C.T. state (337 nm-*a*) or 4*f* levels (594.5 nm-*b* and 582.0 nm-*c*).

Selective Excitation of the Nd^{3+} Emission

Experimental

The luminescence study was performed on powders prepared as described previously (*1*). Luminescence spectra and decays were recorded under excitation by a dye laser pumped by a pulsed nitrogen laser. The emission was detected by an InGaAsP photomultiplier Varian, and the signal was fed into a PAR Model 162/165 boxcar.

Results

The intense charge transfer band with maximum at about 300 nm extends in the visible up to about 500 nm (*1*). For absorption of the incident radiation into this band all Nd^{3+} sites are excited. Figure 5a shows the $^4F_{3/2} \rightarrow {}^4I_{9/2}$ emission for excitation at 337 nm at 4 K. The broad lines observed for small Nd^{3+} concentration in $CaGa_2S_4$ split into two components. The presence of shoulders indicate some disorder in the structure.

Selective excitation of the Nd^{3+} ions in different sites was attempted using a rhodamine laser whose wavelength range, 580–600 nm, covered that of the intense $^4I_{9/2} \rightarrow {}^4G_{5/2}$, $^2G_{7/2}$ absorption lines. The intensity variations according to the excitation wavelength allow one to separate the emission lines into two groups (labeled A and B, Figure 5b and 5c).

Comparison of the time-resolved spectra recorded after 3 and 50 μsec indicates slightly faster decay for the B sites. After about 30 μsec decays of both emissions show an exponential part characterized by very close decay times (A, 57 ± 1 μsec; B, 56 ± 1 μsec) as expected from the great similarity of the available sites. The nonexponential initial part is due to transfer to

neodymium ions in irregular positions or other defects. For excitation into the charge transfer band, the intensities of the A and B emissions are comparable. Since the probability of energy transfer between the two kinds of ions at 4 K is low, it can be concluded that most neodymium ions are equally distributed in two sublattices, in agreement with the X-ray diffraction study.

Conclusions

The distribution of the Nd^{3+} ions in the sulfur lattice sites of $NaNdGa_4S_8$ accounts for the very low concentration quenching observed:

—(i) Cross-relaxation processes are reduced by the large distance between the nearest neighbors (6.07 Å between Nd_1 and Nd_2 ions along *c*) which reduces multipolar interactions and by the absence of common apices between the coordination polyhedra which lessens exchange interactions.

—(ii) The two nearest neighbors lie in different types of sites so the shift of the energy levels decreases the probability of the $^4F_{3/2} \rightarrow {}^4I_{9/2}$, $^4I_{9/2} \rightarrow {}^4F_{3/2}$ energy transfer which will require phonon-assisted processes. The shortest distance between Nd^{3+} ions of the same sublattice amounts to 7.74 Å. Consequently despite the high oscillator strengths of *f–f* transitions in sulfides, the energy losses by migration to defects are considerably reduced.

Acknowledgment

One of us thanks the Conselleria d'Educació i Ciéncia del Pais Valenciá for financial support.

References

1. R. IBANEZ, A. GARCIA, C. FOUASSIER, AND P. HAGENMULLER, *J. Solid State Chem.* **53,** 406 (1984).
2. W. LENTH, H. D. HATTENDORF, G. HUBER, AND F. LUTZ, *Appl. Phys.* **17,** 367 (1978).
3. F. AUZEL, *Mater. Res. Bull.* **14,** 223 (1979).
4. B. EISENMANN, M. JAKOWSKI, W. KLEE, AND H. SCHÄFER, *Rev. Chim. Miner.* **20,** 255 (1983).
5. G. S. SMITH AND R. L. SNYDER, *J. Appl. Crystallogr.* **12,** 60 (1979).
6. G. M. SHELDRICK, "SHELX 76, Program for Crystal Structure Determination," University of Cambridge (1976).
7. J. A. IBERS AND W. C. HAMILTON, Eds., "International Tables for X-ray Crystallography" Vol. IV, Kynoch Press, Birmingham (present distributor Reidel, Dordrecht) (1974).
8. R. ROQUES, R. RIMET, J. P. DECLERCQ, AND G. GERMAIN, *Acta Crystallogr. Sect. B* **35,** 555 (1979).
9. W. KLEE AND H. SCHAEFER, *Rev. Chim. Miner.* **16,** 465 (1979).
10. D. L. DEXTER AND J. H. SCHULMAN, *J. Chem. Phys.* **22**(6), 1063 (1954).
11. M. INOKUTI AND F. HIRAYAMA, *J. Chem. Phys.* **43**(6), 1978 (1965).